Tunable and switchable soft adsorption of polymer-coated microparticles on a flat substrate

Giuseppe Boniello, Christophe Tribet, Emmanuelle Marie, Vincent Croquette, Dražen Zanchi

Tunable and switchable soft adsorption of polymer-coated microparticles on a flat substrate

Giuseppe Boniello[a,b,*], Christophe Tribet[b], Emmanuelle Marie[b], Vincent Croquette[c], Dražen Zanchi[b,d]

[a] *current affiliation: Chemical and Biomolecular Engineering, University of Pennsylvania, Philadelphia, PA, 19104, USA*
[b] *Ecole Normale Supérieure-PSL Research University, Dpt Chimie, Sorbonne Universités - UPMC Univ. Paris 06, CNRS UMR 8640, 24 rue Lhomond, 75005 Paris, France*
[c] *Ecole Normale Supérieure, Département de Physique and Département de Biologie, Laboratoire de Physique Statistique UMR CNRS-ENS 8550, 24 rue Lhomond, 75005 Paris, France*
[d] *Université de Paris VII Denis Diderot, 5 Rue Thomas Mann, 75013 Paris, France*

Abstract

Soft adhesion to a horizontal flat substrate of micron-sized colloids coated by a controlled molar fraction f of PLL-g-PNIPAM is tuned and triggered by controlling the temperature of the sample. This is because PNIPAM is a thermo-responsive polymer, which undergoes a phase transition at a LCST (lower critical solution temperature) $T_c = 32 \pm 1°\mathrm{C}$. In order to capture the very final events before the immobilization of colloids the T-ramp protocol is designed: the particles suspension is injected in cell at room temperature, the temperature is increased at constant rate up to $38°\mathrm{C} > T_c$, and kept constant until the end of the acquisition. Attraction between beads and the flat substrate is thereby triggered when crossing the critical temperature T_c. Both ascending and descending ramp experiments are done in order to access both adsorption and desorption kinetics. 3-D beads motion is real-time tracked using slightly defocused microscopy in parallel illumination. We use track records to have access at pre-adsorption diffusion coefficient and to characterize adsorption and desorption dynamics. Present results corroborate that adsorption is controlled by PNIPAM doping, and indeed dominated by rolling and memory (aging) effect

*Corresponding author
Email address: gboni@seas.upenn.edu (Giuseppe Boniello)

on the contact domain. On the other hand, the desorption kinetics is independent of doping. Moreover, the sharpness (in T) of the PNIPAM transition is quantified in a set of experiments at different ramp speed. We show that the transition smearing can reach up to $\pm 1°$C for higher PNIPAM coverage, while it is not detectable for the lowest ones. The combination of all these observations paves the way to practical applications. We will discuss, for instance, a soft adhesion-based method to sort and separate colloids in microfluidic channels.
Keywords: Colloids, temperature responsive polymers, PNIPAM, colloidal sorting, adsorption, desorption

---

1. Introduction

Functionalized colloids are micrometric or nanometric particles whose surface has been modified to introduce selected properties. For example, continuous or discrete sticky regions can be added to induce attractive interactions with other particles [1, 2, 3] and/or with a substrate [4, 5]. Self-assembling of particles attracts increasing interest for the possibility of bottom-up designed composite materials [6, 7]. Assembling dynamics in modulated external fields (temperature, light, pH, magnetic fields) enables to trigger the interaction resulting in interesting new out-of-equilibrium structures and patterns [8, 9]. On the other hand, comprehension of adsorption properties of sticky colloids on surfaces are relevant pre-requisite for their potential use in biology, as bacterial adhesion [10, 11] and the design of biofouling resistant devices [12]. Controlled interactions with the solid phase can be also involved in a field-flow approach [13, 14] as separation technique for purification of colloidal suspensions (e.g., to sort particles as a function of surface composition or patches architecture). A very common tool for reversibly adhesive colloids are DNA strands [15, 16]. Beyond self-assembly, dynamics of adsorption and desorption processes on flat substrate have been addressed [17, 18, 19]. Brownian dynamics of colloids sticking on a flat surface have been studied in a number of approaches [19, 20]. Observations by optical microscopy in a finely tuned tempera-

ture range show thermo-sensitive behaviors around DNA melting temperature. Here we propose a different approach for both surface functionalization and temperature-dependent study. It is characterized by high experimental accessibility and efficiency, ideal for affordable devices in large scaled applications. Grafted PLL-g-PNIPAM [21] functionalizes reversibly T-responsive particles. Employing different optical video microscopy methods we study pre-adsorption dynamics, adsorption and desorption kinetics for particle populations having different PLL-g-PNIPAM surface coverage. Unlike the classical approach [19] in which the cell is finely thermostated and the dynamics is recorded for each temperature separately, we adopt a "T-ramp" technique where the particle motion is recorded for an increasing (or decreasing) temperature at constant rate. These results confirm and give strength to the "rolling-aging model" that we previously introduced in a recent paper [22].

2. Materials and methods

Sample preparation. Polymer-coated particles are obtained following the protocol proposed in ref. [23]. Commercial silica beads (Bangs Laboratories, SS03N) with diameter of $0.96\mu m$ are dispersed in 1M sodium hydroxide (NaOH) solution and dialysed against water (Slide-A-Lyzer, M_W cutoff 3500 kDa, Thermo Scientific). The solution is diluted in 0.01 M Phosphate-buffered Saline (PBS) solution. Particle are coated by mixing $22\mu L$ of colloidal suspension in PBS and $100\mu L$ of polymer solution (PLL-g-PEG + PLL-g-PNIPAM) at a concentration of $10g.L^{-1}$. (PLL: $M_w = 15000-30000g.mol^{-1}$, grafting density 20%; PEG: $M_w = 20000g.mol^{-1}$, $R_g = 6.9$ nm; PNIPAM: $M_w = 7000g.mol^{-1}$, $R_g = 3.8$ nm). Surface coating is simply achieved because of the electrostatic interaction between the anionic silica surface (after treatment in NaOH) and the cationic PLL backbone of the polymers [23]. Polymer chains adsorb on the particle surface up to saturation density. The surface coverage $f\%$ of the thermo-responsive PLL-g-PNIPAM (which, for the sake of this work, mediated the particle-substrate interaction) is controlled by the concentration of poly-

mer solution. $(100-f)\%$ of PLL-g-PEG is added to ensure steric repulsion and dilute active polymer. Such a final suspension is incubated for 30 min. Polymer excess is removed by 5 centrifugation cycles (1,800g for 5 min) replacing the supernatant by deionized water. DLS measurements [3] confirmed that colloidal suspensions at any f are stable up to PNIPAM cloud temperature ($T_c = 32°$C). Zeta-potential measurements of colloids at different PNIPAM surface coverage were reported in Ref. [23]. The flat substrate consists in a commercial borosilicate glass slides (thickness=0.17 mm) coated following the same procedure. Slight topology variation within the vision stage are lower that z-coordinate precision of experimental apparatus (less than 10nm), as revealed by precise measurement of z-position of immobile, surface-adsorbed beads. Slides are cleaned in ethanol and plunged in a 1M NaOH for 30 min in ultrasonic bath. They are rinsed with deionized water and used as a bottom support for a microfluidic channel. A bi-adhesive tape with controlled thickness (50μm) is used as a spacer, and the cell is closed by a mylar film (top boundary). Glass slides are functionalized by injecting polymer solution (PLL-g-PEG, PLL: $M_w = 15000-30000 g.mol^{-1}$, grafting density 20%; PEG: $M_w = 20000 g.mol^{-1}$, $R_g = 6.9$ nm, $1 g.L^{-1}$ in 0.01M Phosphate-buffered Saline solution) in the channel. After 30 min incubation the cell is rinsed with deionized water to remove polymer solution and polymer excess, and dried with compressed air. Zeta-potential of PLL-g-PEG coated glass slides are of the order of -10mV [24, 25]. A colloidal suspension of particle in PBS ($\sim 20\mu$L, particle concentration 0.1 g/L), with a desired PNIPAM surface coverage f, is injected in the microfluidic channel at room temperature $T = 23-25°$C. The sample is observed in a T-ramp by optical microscopy with the methods described in the following section. Cell preparation is repeated for particle populations at different f in the range $2\% - 100\%$.

Methods. The sample is placed on a Temperature Controlled Microscope Stage (Linkam PE94). The stage is initially set at $T = 26°$C. Acquisitions are obtained swiping the stage temperature at a constant rate ($10°$C/min, unless otherwise noted) in both increasing and decreasing directions. The advantage of

the "T-ramp" consists in exploring any temperature in a range around PNIPAM cloud temperature ($T_c = 32°C$) even without a fine control on experimental parameters. This method is successful and reliable because it allows to get rid of: i) experimental uncertainty on stage temperature; ii) uncertainty on sample temperature, different from the previous one because of thermal inertia; iii) uncertainty on PNIPAM cloud temperature T_c. A typical acquisition contain 40-50 particles in the field of view that are tracked simultaneously. Several sets of data are obtained from a single sample.

i) Pre-adsortion dynamics. The motion of the particles is 3-D tracked in real time using a PicoTwist apparatus and PICOUEYE software tracking (www.picotwist.com). Each particle is observed in slightly defocused microscopy in parallel illumination, resulting in interference rings (Fig. 1a). Comparing ring size to an initial calibration profile (Fig. 1b) allows to extract the vertical position with a 10 nm resolution[26, 27]. Intensity center-of-mass of images as in Fig. 1a gives position on the horizontal plane with a subpixel resolution of $\sim$ 5nm. Temporal resolution is 50 frames/s. Trajectories x,y,z are statistically analyzed in order to extract Mean Square Displacements and diffusion coefficients in different time windows Δt before adsorption.

ii) Adsorption kinetics. Acquisition in T-ramp (starting temperature $T_i = 26°C$, final temperature $T_f = 38°C$, temperature rate $10°C/min$, unless otherwise noted) allows to follows 40-50 particles in an approximately 150×120 px^2 frame (surface coverage of the flat substrate $0.5 - 0.6\%$). At T_i all the particles fluctuate around an average position because of thermal motion. No drift or external flow are present. At $T_c = 32°C$, the particles start progressively to stop because of PNIPAM-mediated adsorption on the flat substrate. The acquisition runs until no thermal motion is detected, meaning that all the tracked beads are adsorbed. The final frames give the positions of each particle when adsorbed (Fig. 2a). Particles positions at any time t are compared with final positions: if there is correspondence the particle is considered adsorbed at time t. This analysis is easily implemented by an image correlation algorithm. The recorded movies are converted to binary masks (1: particle, 0: background).

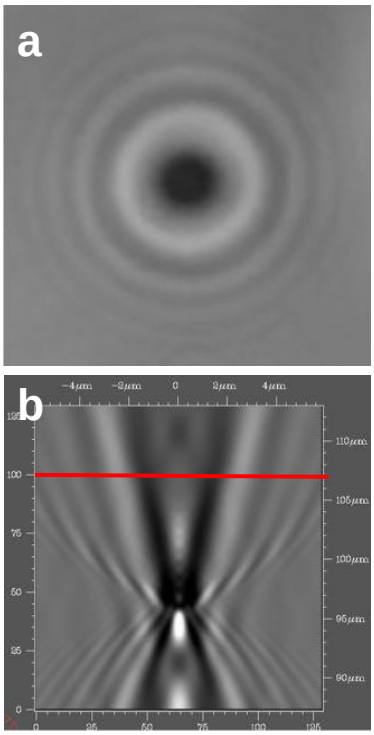

Figure 1: Principles of PICOUEYE tracking analisys. (a) Typical image of a slightly-out-of-focus particle, with characteristic interference rings. (b) Calibration profile giving interference rings width at different vertical positions (relative distance sample-objective). Red line highlights vertical position corresponds to picture in (a).

We calculate:

$$G(t) = \frac{\sum_{x,y} I(t)I(t_f)}{\sum_{x,y} I^2(t_f)} \tag{1}$$

where $\sum_{x,y}$ stands for the sum of all the pixel values on the same resulting image. The correlation function increases when more particles achieve their final position (Fig. 2b). Getting rid of small fluctuation, $G(t)$ give us the cumulative distributions of adsorption times (Fig. 2c), i.e. the fraction $P_a(t)$ of particles attached at the substrate as a function of time [22].

iii) Desorption kinetics. The same principle as above is used for the inverse experiments. Initial temperature is set at $T_i = 36°$C. As initial condition, all the particles in the frame of view are adsorbed on the substrate and have

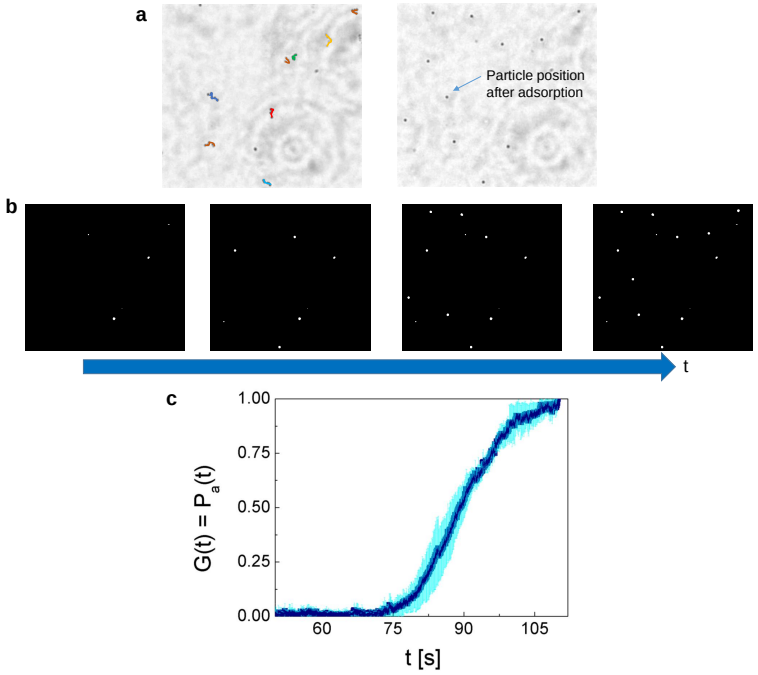

Figure 2: Adsorption kinetics tracking. (a) Extract of video tracking under optical microscopy before (left) and after (right) adsorption. Trajectories in (x,y) plane are recorded. (b) Detail of the algorithm that, among all the particles present in the visible frame ($150\times120px^2$), identifies only the ones adsorbed (white dots) at each time t via image correlation. (c) Intensity profile (blue line) vs. time extracted from pictures as in (b), normalized by intensity at the end of the acquisition. $G(t)$ (Eq. 1 estimates the fraction $P_a(t)$ of adsorbed particles with respect to the total number of tracked ones. Light blue region indicates a confidence interval for the measurement.

fixed position. Temperature is decreased at a constant rate (temperature rate: $10°C/min$) and left at 26°C. Acquisition lasts as far as all the particles are released, showing appreciable motion. The recorded movies are converted to binary masks (1: particle, 0: background). Each frame is compared with the initial one via image correlation. Correlation functions in this case decrease as particles desorb from the substrate. The analysis is here limited to three significant coatings: low ($f = 2\%$), medium ($f = 20\%$) and high ($f = 90\%$) amounts of PNIPAM on the surface.

3. Experimental results

Pre-adsorption dynamics. Particle tracking techniques provide the full particle trajectory in the 3 directions (horizontal plane x, y and vertical particle-substrate distance z) along all the acquisition in the temperature ramp. We already used these information, for instance, to track particle vertical position before adsorption [22] or rocking dynamics after adhesion [3]. Here we integrate previous results observing pre-adsorption dynamics in different temporal windows Δt, but all ending at the adsorption time ($t = t_0$). Fig. 3 shows the Mean Square Displacements (MSDs) for a representative particle ($f = 50\%$, in the middle of the experimental range of surface coverage). When the MSD is sampled over a long Δt ($\Delta t = 33.3$s, green points) we observe a linear curve, characteristic of Brownian diffusion. If we reduce the analysis to times closer to adsorption time ($\Delta t = 16.7$s, blue points) MSD is still linear, but with a lower slope (i.e., a lower diffusion coefficient). Diffusion is hindered by the presence of a solid boundary [28], and by more frequent particle-substrate interactions. Slopes decreases when we reduce Δt ($\Delta t = 10.0$s, red points). In the very last few seconds before adhesion ($\Delta t = 3.3$s, black points) MSD shows a plateau.

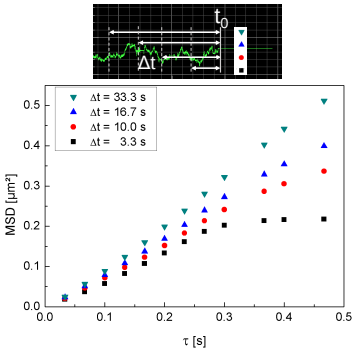

Figure 3: MSDs of a PLL-g-PNIPAM coated particle ($f = 50\%$) before adsorption (at time $t = t_0$). Trajectories are extracted in different time windows Δt ($\Delta t = 3.3, 10, 16.7, 33.3$ s), all ending at t_0.

Adsorption and desorption kinetics. In our previously reported work we an-

alyzed and modeled the curves of adsorbed particles in the full surface coverage range ($2\% < f < 100\%$) in a temperature ramp at a constant rate [22]. We want now to measure the effect of the PNIPAM collapse phase transition kinetics on the adsorption and desorption dynamics within a given T-ramp. Namely, in our previous work, it was assumed that in all cases the PNIPAM conformational changes occur instantaneously in regard to rolling and sticking processes during the T-ramp. Here, we provide new insights on the effect of different ramps. For the sake of discussion, we limit the analysis at two representative values of f ($f = 90\%$, $f = 2\%$) and two ramps: fast ($10°$C/min) and slow ($1°$C/min). Results are reported in Fig. 4a and show different behaviors for the two surface coverage. At $f = 90\%$ we have a quick adsorption after PNIPAM transition, since sticky patches cover almost completely the colloid. Instantaneous adsorption is clearly observed with the fast ramp ($10°$C/min, black curve in Fig. 4a). A slower ramp ($1°$C/min, gray curve in Fig. 4a) doesn't change the interaction, but only smeared PNIPAM transition in a wider time frame. Full particle adsorption is delayed by approximately 1 minute when the sample temperature is increased of $1°$C. On the contrary, particle with lower surface coverage don't show such a delay. The two curves at different temperature rates overlap within experimental error (dark and light red curves in Fig. 4a), indicating much slower smearing of PNIPAM transition temperature than in the case of high coverage f.

A decreasing T-ramp allows to explore desorption kinetics (Fig. 4b). We use three particle populations with different f: 90% (black points), 20% (light blue points), 2% (red points). The acquisition starts at $T = 38°$C with all the particle adsorbed on the substrate (fraction of adsorbed particle $P_a(t_0) = 1$) and ends when all the accessible particles are released ($P_a(t_f) = 0$). No relevant differences are found between different polymer coverage. All the particle populations desorb with the same kinetics. This result tell us that desorption only depends on PNIPAM state: when the transition from collapsed to coil states occurs, colloids are not sticky anymore and leave the substrate. Adsorption was tuned by rolling of the particle, looking for sticky patches (for larger f, patched

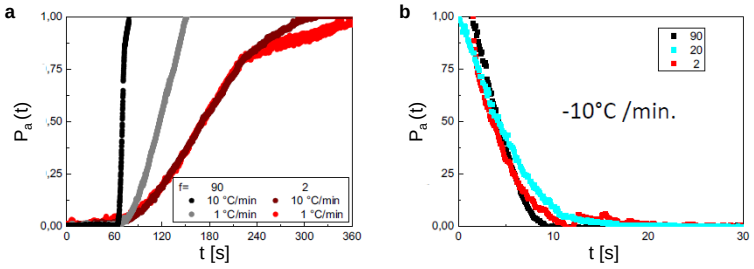

Figure 4: (a) Fraction of adsorbed particles as a function of time in increasing T-ramps at different rates, 10°C/min (dark colors), 1°C/min (light colors), for two representative surface coverage f: 90% (black/gray) and 2% (red). (b) Fraction of adsorbed particle as a function of time in decreasing T-ramp (rate 10°C/min) for three particle populations: high ($f = 90\%$, black), medium ($f = 20\%$, light blue) and low ($f = 2\%$, red) surface coverage.

are more frequent and adhesion faster). In contrast, the fast and uniform release of particles suggests that rolling or rocking dynamics are not involved prior to desorption.

4. Discussion

Temperature-sensitive polymer (PLL-g-PNIPAM) induces reversible particle adsorption and desorption as a function of the sample temperature. The PLL-g-PNIPAM surface coverage f is able to tune adsortion kinetics (but not desorption one): larger is f, faster is the adhesion. We recently provided a model to describe this phenomenon and fit experimental curves [22]. The model accounts for rolling and aging effect in soft adhesion: at lower f the colloids spend more time in proximity of the substrate before finding a sticky polymer patch. We divide the particles into three populations, corresponding to the three stages of a particle's "life". The first is the population of untethered colloids, represented by the probability $P_b(t)$. The second population represents the rolling colloids, $P_r(t)$, while the third population of colloids is in arrest, $P_a(t)$. Thus, the rate equations are written:

$$\dot{P}_b = -\kappa P_b + k_{\text{off}}\,\rho(t/\tau^*)P_r$$

$$\begin{aligned} \dot{P}_r &= \kappa P_b - [k_{\text{off}}\,\rho(t/\tau^*) + \varphi(T)\,k\,g(t/\tau^*)]\,P_r \\ P_a &= 1 - P_b - P_r\ , \end{aligned} \tag{2}$$

where κ is the free sedimentation rate and corresponds to the fraction of particles absorbed per unit time by a totally absorbing sink [29]. The term k_{off} is the re-dispersion rate of rolling colloids, and k is the irreversible stopping rate of rolling colloids. The typical time scale for contact aging is τ^*, and allows us to write aging functions $\rho(x) = \exp(-x)$ and $g(x) = 1 - \rho(x)$. Initial conditions correspond to all the colloids dispersed in the bulk: $P_b(0) = 1$, $P_r(0) = P_a(0) = 0$. The final state is $P_a(t_f) = 1$. See ref. [22] for full details. The results in this work go in the same direction. They confirm previous observation and strengthen the rolling-aging model. The model has been designed under the assumption of an instantaneous trigger of PNIPAM repulsion/attraction at the PNIPAM cloud temperature ($T_c = 32°\text{C}$). It can be accounted by a step function for PNIPAM response: $\varphi(T) = 0$ for $T < T_c$, and $\varphi(T) = 1$ for $T > T_c$. This approximation works when the temperature transition around T_c is much faster than adsorption (temperature transition time $t_{Temp} \gg \tau^*$), i.e. for slow adsorption (low f) or fast T-ramp (10°C/min). As a result, adsorption profiles at $f = 2\%$ are independent of T-ramp (Fig. 4a, red lines). Otherwise, when $t_{Temp} \sim \tau^*$, the response function becomes smeared:

$$\varphi(\frac{T - T_c}{\Delta T}) = \frac{\exp\frac{T-T_c}{\Delta T}}{\exp\frac{T-T_c}{\Delta T} + 1}. \tag{3}$$

This translates in different adsorption profiles for fast and slow T-ramps for $f = 90\%$ (Fig. 4a, black/gray lines).

Desorption doesn't show a dependence of PNIPAM coverage f on colloids surface. Rolling and soft contact are not involved, but particles are released when PNIPAM tethers become non-sticky (Fig. 4b). This depends on sample temperature, but not on tethers density. For desorption a simple rate equation describes the phenomenon at any f:

$$\dot{P}_a = -\kappa_T P_a, \tag{4}$$

where κ_T is the re-dispersion rate dictated by tethers conditions.

Application: sorting in microfluidic channel. Strong dependence of adsorption rate on f, reversibility of the effect in temperature, together with fast and f-independent desorption rate are precious ingredients for designing a separation device for patchy colloids.

The principle is depicted in Fig. 5: a suspension containing a mixture of colloids with different patchy patterns is injected at constant flow into a separation device containing PEG coated silica horizontal substrate, subject to sedimentation. At the beginning, the temperature is below T_c. At some time, the temperature is rapidly raised above T_c. Colloids with different patchiness will take different times to adsorb. After a sticky time τ_s the temperature is dropped below T_c. All particles are released and continue the flow during the free time τ_f. The process is repeated as long as the device requires (depending on its length and the flow speed). The crucial point is that τ_s and τ_f can be tuned in order to get the best separation. For example, if we want to separate particles heaving $f = 50\%$ from the ones with $f = 2\%$, the sticking time must be chosen in a way that most of "50s" get stuck but most of "2s" continue to flow.

The same separation technique can be used for resolving particles with same f, but with different patch patterns. For this purpose, we use the fact that particles mostly roll while they are sticky, and merely jump while they are free. Fig. 6a-d illustrates an extreme case in which two particles with same coverage f but different coverage patterns (N random patches vs complete de-mixing, N=1). The trail (red) that the contact domain draws on the colloid surface is continuous in the case of rolling (crawling) (Fig. 6b-e) and is composed of discrete drops in the case of jumping (Fig. 6c-f). It is well known that the first passage times are radically different in the two cases [30, 31]. In our separation device, we can tune between the two: if we want continuous trails to dominate, we will make longer τ_s. On the contrary, if we want discontinuous searching, we prefer short τ_s. The free time should be adjusted in both cases to allow most of particles to desorb, otherwise no material can be detected at the end.

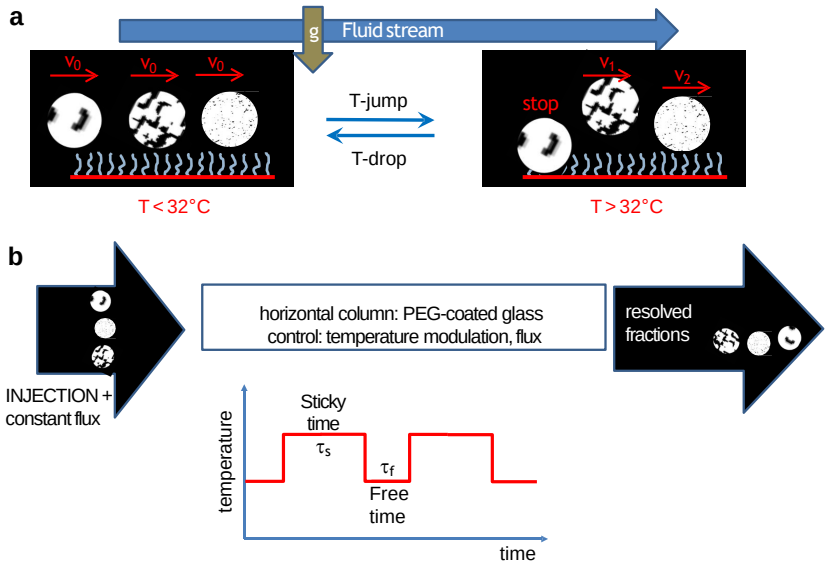

Figure 5: Application of soft adhesion in particle sorting/separation. (a) The separation device is a microfluidic channel with horizontal PEG-coated glass substrate, placed in a temperature-controlled environment, rapidly tunable and programmable. The flow v_0 is controlled and kept constant during separation. (b) The separation procedure is achieved by a sequence of T-jump/T-drop cycles with tunable sticky time τ_s and free time τ_f.

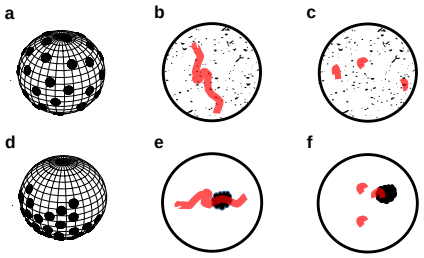

Figure 6: Rolling and jumping for particles with same coverage f but different patterns. (a, d) Schematic of different patches distributions. (b, e) Continuous trails (red lines) for particles during rolling. (c, f) Discrete drops for particles during jumping. Particles in (a-c) encounter sticky tethers more often then particles in (d-f).

5. Conclusions

The present work reports further experimental results on colloid-substrate adhesion for microparticles coated by a controlled amount f of temperature-responsive polymer chains (PLL-g-PNIPAM). We used 3-D real time tracking within an ascending and descending temperature ramp around the polymer collapse temperature, triggering the stickiness of the particles. Soft adhesion is reversible and can be finely tuned by f. The combination of new observations (pre-adsorption diffusion, adsorption smearing at different T-ramps, desorption) strengths our model, confirming that soft adhesion is controlled by rolling and aging effects. Furthermore, on the basis of our results, we propose a simple strategy for separation of colloids with soft sticky patches. Separation with respect to both the overall surface patch density and the patch pattern is discussed.

6. Acknowledgments

This work was supported by ANR DAPPlePur 13-BS08-0001-01 and program "investissement d'avenir" ANR-11-LABX-0011-01.

References

References

[1] B. A. Grzybowski, C. E. Wilmer, J. Kim, K. P. Browne, K. J. Bishop, Self-assembly: from crystals to cells, Soft Matter 5 (6) (2009) 1110–1128.

[2] S. R. Risbud, J. W. Swan, Dynamic self-assembly of colloids through periodic variation of inter-particle potentials, Soft matter 11 (16) (2015) 3232–3240.

[3] G. Boniello, J. Malinge, C. Tribet, E. Marie, D. Zanchi, Reversible and dynamical control of aggregation and soft adhesion of t-responsive polymer-coated colloids, Colloids Surf., A (2017) – doi:https://doi.org/10.1016/j.colsurfa.2017.04.011.

URL http://www.sciencedirect.com/science/article/pii/S0927775717303424

[4] R. D. Duffadar, J. M. Davis, Dynamic adhesion behavior of micrometer-scale particles flowing over patchy surfaces with nanoscale electrostatic heterogeneity, Journal of colloid and interface science 326 (1) (2008) 18–27.

[5] M. M. Santore, N. Kozlova, Micrometer scale adhesion on nanometer-scale patchy surfaces: adhesion rates, adhesion thresholds, and curvature-based selectivity, Langmuir 23 (9) (2007) 4782–4791.

[6] J. Largo, P. Tartaglia, F. Sciortino, Effective nonadditive pair potential for lock-and-key interacting particles: The role of the limited valence, Phys. Rev. E 76 (1) (2007) 011402. doi:10.1103/PhysRevE.76.011402.

[7] F. Sciortino, E. Zaccarelli, Reversible gels of patchy particles, Curr. Opin. Colloid Interface Sci. 15 (6) (2011) 246–253. doi:10.1016/j.cossms.2011.07.003.

[8] R. Straube, M. Falcke, Reversible clustering under the influence of a periodically modulated binding rate, Phys. Rev. E 76 (1) (2007) 010402. doi:10.1103/PhysRevE.76.010402.

[9] K. J. M. Bishop, B. A. Grzybowski, Localized chemical wave emission and mode switching in a patterned excitable medium, Phys. Rev. Lett. 97 (12) (2006) 128702. doi:10.1103/PhysRevLett.97.128702.

[10] S. Gon, K.-N. Kumar, K. Nüsslein, M. M. Santore, How bacteria adhere to brushy peg surfaces: clinging to flaws and compressing the brush, Macromolecules 45 (20) (2012) 8373–8381. doi:10.1021/ma300981r.

[11] T. Vissers, A. T. Brown, N. Koumakis, A. Dawson, M. Hermes, J. Schwarz-Linek, A. B. Schofield, J. M. French, V. Koutsos, J. Arlt, et al., Bacteria as living patchy colloids: Phenotypic heterogeneity in surface adhesion, Science advances 4 (4) (2018) eaao1170.

[12] S. Gon, B. Fang, M. Santore, Interaction of cationic proteins and polypeptides with biocompatible cationically-anchored peg brushes, Macromolecules 44 (20) (2011) 8161–8168. doi:10.1021/ma201484h.

[13] J. C. Giddings, Field-flow fractionation: analysis of macromolecular, colloidal, and particulate materials, Science 260 (5113) (1993) 1456–1465. doi:10.1126/science.8502990.

[14] M. Martin, R. Beckett, Size selectivity in field-flow fractionation: Lift mode of retention with near-wall lift force, J. Phys. Chem. A 116 (25) (2012) 6540–6551. doi:10.1021/jp212414e@proofing.

[15] A. V. Tkachenko, Morphological diversity of dna-colloidal self-assembly, Phys. Rev. Lett. 89 (2002) 148303. doi:10.1103/PhysRevLett.89.148303.

[16] M.-P. Valignat, O. Theodoly, J. C. Crocker, W. B. Russel, P. M. Chaikin, Reversible self-assembly and directed assembly of dna-linked micrometer-sized colloids, Proc. Natl. Acad. Sci. U.S.A. 102 (12) (2005) 4225–4229.

[17] N. Licata, A. Tkachenko, Dynamics of particles with "key-lock" interactions, Europhys. Lett. 81 (4) (2008) 48009.

[18] N. A. Licata, A. V. Tkachenko, Kinetic limitations of cooperativity-based drug delivery systems, Phys. Rev. Lett. 100 (15) (2008) 158102.

[19] Q. Xu, L. Feng, R. Sha, N. Seeman, P. Chaikin, Subdiffusion of a sticky particle on a surface, Phys. Rev. Lett. 106 (22) (2011) 228102. doi:10.1103/PhysRevLett.106.228102.

[20] B. Fang, S. Gon, M.-H. Park, K.-N. Kumar, V. M. Rotello, K. Nüsslein, M. M. Santore, Using flow to switch the valency of bacterial capture on engineered surfaces containing immobilized nanoparticles, Langmuir 28 (20) (2012) 7803–7810. doi:10.1021/la205080y.

[21] I. Luzinov, S. Minko, V. V. Tsukruk, Responsive brush layers: from tailored gradients to reversibly assembled nanoparticles, Soft Matter 4 (4) (2008) 714–725.

[22] G. Boniello, C. Tribet, E. Marie, V. Croquette, D. Zanchi, Rolling and aging in temperature-ramp soft adhesion, Physical Review E 97 (1) (2018) 012609.

[23] J. Malinge, F. Mousseau, D. Zanchi, G. Brun, C. Tribet, E. Marie, Tailored stimuli-responsive interaction between particles adjusted by straightforward adsorption of mixed layers of poly (lysine)-g-peg and poly (lysine)-g-pnipam on anionic beads, J. Colloid Interface Sci. 461 (2016) 50–55. doi:10.1016/j.jcis.2015.09.016.

[24] S. Gon, M. Bendersky, J. L. Ross, M. M. Santore, Manipulating protein adsorption using a patchy protein-resistant brush, Langmuir 26 (14) (2010) 12147–12154.

[25] S. Kalasin, M. M. Santore, Near-surface motion and dynamic adhesion during silica microparticle capture on a polymer (solvated peg) brush via hydrogen bonding, Macromolecules 49 (1) (2015) 334–343.

[26] C. Gosse, V. Croquette, Magnetic tweezers: micromanipulation and force measurement at the molecular level, Biophys. J. 82 (6) (2002) 3314–3329. doi:10.1016/S0006-3495(02)75672-5.

[27] T. R. Strick, J.-F. Allemand, D. Bensimon, A. Bensimon, V. Croquette, The elasticity of a single supercoiled dna molecule, Science 271 (5257) (1996) 1835. doi:10.1126/science.271.5257.1835.

[28] J. Leach, H. Mushfique, S. Keen, R. Di Leonardo, G. Ruocco, J. M. Cooper, M. J. Padgett, Comparison of faxén's correction for a microsphere translating or rotating near a surface, Phys. Rev. E 79 (2009) 026301. doi:10.1103/PhysRevE.79.026301.

[29] H. Brenner, The slow motion of a sphere through a viscous fluid towards a plane surface, Chem. Eng. Sci. 16 (3-4) (1961) 242–251.

[30] N.-K. Lee, A. Johner, F. Thalmann, L. Cohen-Tannoudji, E. Bertrand, J. Baudry, J. Bibette, C. M. Marques, Ligand- receptor interactions in chains of colloids: When reactions are limited by rotational diffusion, Langmuir 24 (4) (2008) 1296–1307.

[31] H.-X. Zhou, Brownian dynamics study of the influences of electrostatic interaction and diffusion on protein-protein association kinetics, Biophysical journal 64 (6) (1993) 1711–1726.

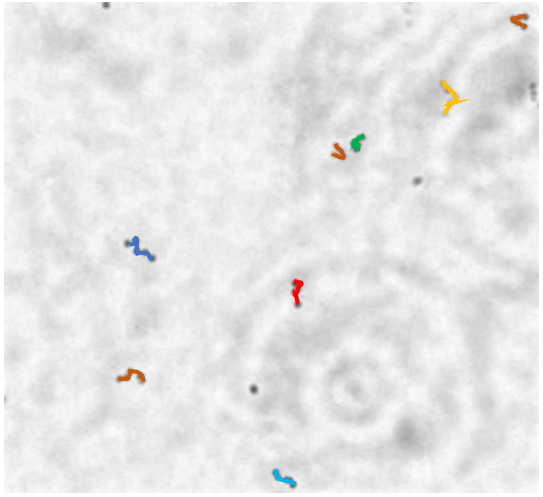

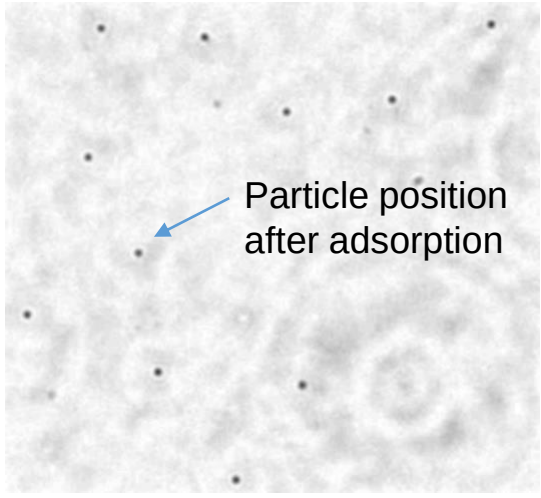
Particle position
after adsorption


t